Theoretical description of the spatial dependence of sickle hemoglobin polymerization

Huan Xiang Zhou and Frank A. Ferrone
Department of Physics and Atmospheric Science, Drexel University, Philadelphia, Pennsylvania 19104 USA

ABSTRACT We have generalized the double nucleation mechanism of Ferrone et al. (Ferrone, F. A., J. Hofrichter, H. Sunshine, and W. A. Eaton. 1980. *Biophys. J.* 32:361–377; Ferrone, F. A., J. Hofrichter, and W. A. Eaton. 1985. *J. Mol. Biol.* 183:611–631) to describe the spatial dependence of the radial growth of polymer domains of sickle hemoglobin. Although this extended model requires the consideration of effects such as monomer diffusion, which are irrelevant to a spatially uniform description, no new adjustable parameters are required because diffusion constants are known independently. We find that monomer diffusion into the growing domain can keep the net unpolymerized monomer concentration approximately constant, and in that limit we present an analytic solution of the model. The model shows the features reported by Basak, S., F. A. Ferrone, and J. T. Wang (1988. *Biophys J.* 54:829–843) and provides a new means of determining the rate of polymer growth. When spatially integrated, the model exhibits the exponential growth seen in previous studies, although molecular parameters derived from analysis of the kinetics assuming uniformity must be modified in some cases to account for the spatially nonuniform growth. The model developed here can be easily adapted to any spatially dependent polymerization process.

INTRODUCTION

The primary event in creating a viscous gel from deoxygenated sickle hemoglobin is the formation of polymers which occurs with great rapidity after an apparent delay. Nucleation-controlled polymerization was identified as an element in this process when the extraordinarily high reaction order was first observed (Hofrichter et al., 1974; Malfa and Steinhardt, 1974). However, classic polymer nucleation theories as elaborated by Oosawa and Asakura (1975) and modified for nonideality (Eaton and Hofrichter, 1978) predicted a simple t^2 time dependence rather than the observed exponential reaction. Relaxation of the nucleation assumption to make the reaction sequential in time accelerates the time course at the expense of the high concentration dependence (Firestone et al., 1983; Goldstein and Stryer, 1986; Rangarajan and de Levie, 1983).

A pivotal observation breaking this impasse was that the delay time exhibited stochastic fluctuations when polymerization was observed in small volumes, whereas the growth rate thereafter was entirely reproducible (Ferrone et al., 1985*a*; Ferrone et al., 1980; Hofrichter, 1986). This signaled the incompatibility of a theory in which each polymer was formed independently, because fluctuations would be associated with one (or at most a few) molecular events, and yet a large number of polymers were formed.

By postulating a second polymer formation pathway, involving the nucleation of new polymers onto the surface of previously formed polymers, the high autocatalysis and concentration dependence could be reconciled in a double nucleation mechanism that naturally provided for the proliferation of polymers from a single molecular event (Ferrone et al., 1985 *b*; Ferrone et al., 1980). The model was found capable of describing the polymerization process over the entire realm of observations, using thermodynamically motivated reasonable parameters.

However, this mechanism is intrinsically spatially nonuniform. Because the secondary nucleation forms polymers attached to other polymers, a network is formed. Evidence for the existence and structure of this polymer network, or domain, has come from optical microscopy (Beach et al., 1988; Hofrichter, 1979; Hofrichter et al., 1976; Mickols et al., 1988; Mickols et al., 1985; Sunshine et al., 1982; White and Heagan, 1970) and electron microscopy (White and Heagan, 1970). These networks were firmly established as part of the fundamental mechanism by the observation that the kinetics of polymerization became stochastic only when a single domain was formed, implying that the entire cluster was created from a single molecular event (Ferrone et al., 1985*a*; Ferrone et al., 1980; Hofrichter, 1986).

H. X. Zhou's present address is Laboratory of Chemical Physics, National Institute of Diabetes and Digestive and Kidney Diseases, National Institutes of Health, Bethesda, MD 20892.

0006-3495/90/09/695/09 $2.00

Even if the polymers spawned by the heterogeneous process do not remain attached, the resulting polymerization process must be spatially dependent. The double nucleation model was originally formulated in a spatially uniform way because the only kinetic data available were spatially averaged over the entire domain. Thus, the assumption of uniformity was reasonable, though clearly temporary. We have recently undertaken an experimental program to investigate the kinetics of formation of domains (Basak et al., 1988; Ferrone et al., 1987). The initial results of that study show domains to originate with considerable circular symmetry. When viewed radially, the domains are approximately gaussian in shape. In time the width as well as the amplitude of the gaussian shape increases (Basak et al., 1988).

In this paper, we show how to account for the natural spatial nonuniformity implicit in the double nucleation model, or any secondary pathway model, without introducing new adjustable molecular parameters. This extended model requires the consideration of effects irrelevant to the spatially uniform description, most notably, monomer diffusion. We find that monomer diffusion into the growing domain can keep the net unpolymerized monomer concentration approximately constant, and in that limit we present an analytic solution. The model shows the features reported by Basak et al. (1988) and, when spatially integrated, exhibits the exponential growth seen in previous studies. Furthermore, this model can be easily adapted to any spatially dependent polymerization process.

The outline of this paper is as follows. First, the equations which govern the spatially nonuniform model are derived. We next present an approximate solution to the model. Then the approximate solution is compared with the salient features seen in polymerization data. Finally we discuss the implications of our findings and future directions.

THE MODEL

In this section, we derive the partial differential equations (summarized in Table 1) which describe spatial and temporal polymer growth from a central point. We begin with the equations for double nucleation (Bishop and Ferrone, 1984; Ferrone et al., 1985*b*; Ferrone et al., 1980; Hofrichter, 1986). The form of these equations is modified slightly because we will only consider events which occur after each homogeneous nucleation event. We then add propagation terms to these equations to account for spatial nonuniformity. The resulting equations are still most appropriate at the initial phase of the reaction, omitting such effects as domain impingement, and lengthening or alignment mechanisms.

TABLE 1 Equations for spatially nonuniform polymerization

$$\frac{\partial c}{\partial t} = -\frac{1}{2}[c_p^+ + c_p^-]\,J(c) + \frac{D}{r}\frac{\partial}{\partial r}\left(r\frac{\partial c}{\partial r}\right) \tag{3}$$

$$\frac{\partial \Delta}{\partial t} = \frac{1}{2}[c_p^+ + c_p^-]\,J(c) \tag{4}$$

$$\frac{\partial c_p^+}{\partial t} = g(c)\Delta - \frac{\alpha}{r}\frac{\partial}{\partial r}(r\,J(c)\,c_p^+) \tag{8}$$

$$\frac{\partial c_p^-}{\partial t} = g(c)\Delta + \frac{\alpha}{r}\frac{\partial}{\partial r}(r\,J(c)\,c_p^-) \tag{9}$$

$$J(c) = k_+(\gamma c - \gamma_s c_s) \tag{2a}$$

$$g(c) = k_+\phi K_{j^*}(\gamma c)^{j^*+1} \tag{2b}$$

For clarity, the spatially uniform model for a single domain is first recapitulated. The concentration of monomers incorporated into polymers, $\Delta(t)$, is related to the concentration of free monomers, $c(t)$, the activity coefficients for the monomer concentration, $\gamma[c(t)]$, and the concentration of polymers, $c_p(t)$, accounted by the concentration of polymer ends by the equation

$$\mathrm{d}\,\Delta/\mathrm{d}t = k_+(\gamma c - \gamma_s c_s)c_p, \tag{1a}$$

in which k_+ is the rate of monomer addition. The monomer concentration at the solubility limit is denoted here by c_s, and the activity coefficient of the monomer solution at that solubility, $\gamma(c_s)$ is denoted simply as γ_s. Assuming that there are no other significant intermediates, Eq. 1a is just the negative of the rate of disappearance of monomers,

$$\mathrm{d}c/\mathrm{d}t = -\mathrm{d}\Delta/\mathrm{d}t. \tag{1b}$$

Finally, new polymers form with the rate,

$$\frac{\mathrm{d}c_p}{\mathrm{d}t} = k_+\frac{\gamma c\,\gamma_{j^*}c_{j^*}}{\gamma_{j^*}^{\ddagger}}\phi\,\Delta. \tag{1c}$$

Here, ϕ represents the fraction of available sites on the surface of the polymer for heterogeneous nucleation, c_{j^*} is the concentration of nuclei of size j^*, γ_{j^*} is the activity coefficient for those nuclei, and $\gamma_{j^*}^{\ddagger}$ is the activity coefficient for the activated complex. It is further assumed that $\gamma_{j^*} = \gamma_{j^*}^{\ddagger}$ and that $c_{j^*} = K_{j^*}(\gamma c)^{j^*}$, where K_{j^*} is a size-dependent equilibrium constant. Note that there is no homogeneous nucleation term in Eq. 1c. For ease of manipulation, the term $k_+(\gamma c - \gamma_s c_s)$ in Eq. 1a, which will be called the elongation rate, will be denoted by $J(c)$,

$$J(c) = k_+(\gamma c - \gamma_s c_s), \tag{2a}$$

and the prefactor of Δ in Eq. 1c, which will be called the heterogeneous nucleation rate will be denoted by $g(c)$,

where

$$g(c) = k_+ \phi K_{j^*} (\gamma c)^{j^*+1}. \quad (2b)$$

To describe the spatially nonuniform growth of a polymer domain it is necessary to describe the concentration at a given point in space as well as time, i.e., $c(t)$ becomes $c(\mathbf{R},t)$, where $\mathbf{R}$ is the position vector of the point under consideration. Because the model will solely deal with radial growth, the concentration of free monomers can be written as $c(r,t)$, where r is the distance from the domain center. Similarly, the concentration of polymerized monomers becomes $\Delta(r,t)$. There are two distinguishable classes of polymer ends. A polymer end at point r, time t, may have originated at shorter distances (i.e., remainder of the polymer resides at values less than r) or it may have originated at longer distances (remainder of the polymer resides at distances greater than r). As polymers grow, the first category will expand the domain, while the second category will fill it up. These two classes of polymer ends are denoted as $c_p^+(r,t)$ and $c_p^-(r,t)$, respectively (see Fig. 1).

The set of differential equations (Eqs. 1 and 2) above, which describe bulk or spatially uniform polymerization, must be modified by the addition of propagation terms, which describe how polymerization at one point in space influences neighboring events. The concentration of monomers $c(r,t)$, for example, will not only change by polymerization, but also by diffusion of monomers into regions depleted of monomers. Thus, if D is the diffusion constant for hemoglobin in solution, then

$$\frac{\partial c}{\partial t} = -\frac{J(c)}{2}[c_p^+ + c_p^-] + \frac{D}{r}\frac{\partial}{\partial r}\left(r\frac{\partial c}{\partial r}\right). \quad (3)$$

Here, D has been assumed to be constant for a given initial concentration; in a recent inelastic light scattering study, Kam and Hofrichter (1986) found that the diffusion constant did not depend on the concentration of polymerized monomers. If the assumption is made that polymers do not diffuse significantly, the rate of change of monomers in solution is no longer matched by the uptake of monomers into polymers. Therefore,

$$\partial\Delta/\partial t = J(c)\,[c_p^+ + c_p^-]/2. \quad (4)$$

The concentration of polymer ends at a given position can change by simple growth of the polymer, which moves the end to a new position. Thus, c_p^+ or c_p^- propagate through monomer addition described by $J(c)$. To derive an equation for the rate of change of polymer ends, we consider an infinitesimally small ring of thickness dr at a distance r from the center (see diagram in Fig. 2). Within the ring $[r, r + dr]$, in time dt, outward growing polymer ends which lie a distance $dl(r)$ from the ring edge $(r + dr)$ will leave the ring. For a single-stranded polymer, this "escape length" can be written as the product of the net growth rate J, the length of each monomer added, α, and the element of time dt, thus:

$$dl(r) = J(r,c)\,\alpha\,dt. \quad (5)$$

For a polymer with n strands, α is the effective length of a single monomer because the addition of n monomers is required to increase the length of the polymer by one monomer. For example, the 14 stranded HbS polymers (Dykes et al., 1978), has $\alpha = (6.4/14)\text{nm} = 0.46$ nm. In addition to polymer ends leaving the ring, the number of polymer ends in the ring will be increased by polymers that enter the ring from smaller sizes. The overall change of polymer ends $c_p^+(r)$, due to elongation of polymers is denoted $(\delta c_p^+)_e$, and satisfies

$$2\pi r\,dr\,(\delta c_p^+)_e = -2\pi r\,dl(r)\,c_p^+(r) + 2\pi\,(r - dr)\,dl(r - dr)\,c_p^+(r - dr). \quad (6)$$

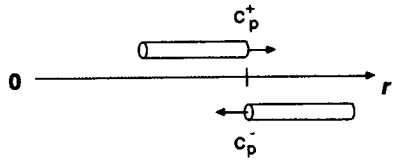

FIGURE 1 The distinction between c_p^+ and c_p^-. Although there is an end of each of the two polymers at the same spatial location, further growth of the c_p^+ polymer will move its end farther from zero, whereas growth of the c_p^- end will move it toward zero.

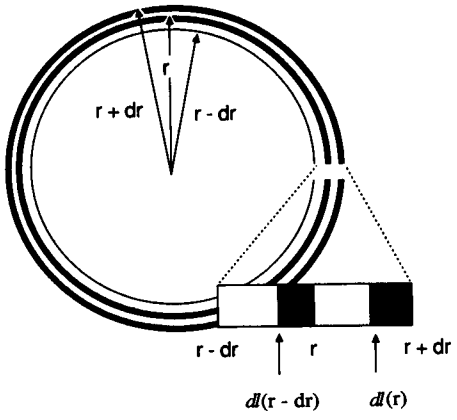

FIGURE 2 Derivation of the net flux of polymers out of and into a ring of radius r. Within the ring $[r, r + dr]$, outward growing polymer ends which lie a distance $dl(r)$ from the ring edge $(r + dr)$ will leave the ring in time dt, whereas polymer ends which lie a distance of $dl(r - dr)$ will enter the ring.

Therefore,

$$(\delta c_p^+)_e = -\frac{\alpha}{r}\frac{\partial}{\partial r}(rJ(c)\, c_p^+)\, dt. \tag{6a}$$

The concentration of polymer ends c_p^+ also increases due to nucleation. That term is given by

$$(\delta c_p^+)_n = g(c)\,\Delta\, dt. \tag{7}$$

Thus, the total rate of change of c_p^+ is:

$$\begin{aligned}\partial c_p^+/\partial t &= [(\delta c_p^+)_e + (\delta c_p^+)_n]/dt \\ &= g(c)\,\Delta - \frac{\alpha}{r}\frac{\partial}{\partial r}(r\,J(c)\, c_p^+).\end{aligned} \tag{8}$$

The equation for c_p^- can be similarly derived, and is

$$\frac{\partial c_p^-}{\partial t} = g(c)\,\Delta + \frac{\alpha}{r}\frac{\partial}{\partial r}(r\,J(c)\, c_p^-). \tag{9}$$

There is an important sign difference in the propagation terms for c_p^+ and c_p^- because c_p^+ propagates by addition in the direction of increasing r, whereas propagation of c_p^- sends polymer ends in the direction of decreasing r. The fact that both directions have been treated equivalently is an assumption about the way in which the heterogeneous nucleation process occurs. A second polymer is visualized as created alongside its parent, so that growth in either direction is possible. This is not rigorously required, and a model with inequivalent treatment of c_p^+ and c_p^- could be formulated if, for example, heterogeneous nucleation possessed a certain polarity.

The above equations have been derived for the particular case of a two-dimensional geometry. In a three-dimensional case, the equations are slightly modified. By straightforward adaptation of the above arguments, it can be shown that

$$\partial\Delta/\partial t = J(c)\,[c_p^+ + c_p^-]/2 \tag{10a}$$

$$\frac{\partial c}{\partial t} = -\frac{J(c)}{2}[c_p^+ + c_p^-] + \frac{D}{r^2}\frac{\partial}{\partial r}\left(r^2\frac{\partial c}{\partial r}\right) \tag{10b}$$

$$\frac{\partial c_p^+}{\partial t} = g(c)\,\Delta - \frac{\alpha}{r^2}\frac{\partial}{\partial r}(r^2\,J(c)\, c_p^+) \tag{10c}$$

$$\frac{\partial c_p^-}{\partial t} = g(c)\,\Delta + \frac{\alpha}{r^2}\frac{\partial}{\partial r}(r^2\,J(c)\, c_p^-). \tag{10d}$$

Note that the equation for Δ is unchanged. The experimental observations of domains that have been made are of thin layer samples of thickness 4–6 μm over areas of the scale of 50–60 μm. Thus, while the two-dimensional limit will not be rigorously applicable through the entire domain growth process, the transition from small three-dimensional growth to a two-dimensional domain above 6 μm would add considerable complexity with little hope of added accuracy or insight, due to the necessity of adding additional assumptions and approximations. Hence, the two-dimensional description will be used in the remainder of this paper.

Because it is possible for a polymer to propagate across the center, c_p^- will be transformed into c_p^+ when it reaches $r = 0$. Hence, the model requires that when the in-growing polymer reaches the center, it abruptly transforms into an out-growing polymer (c_p^+).

The assumption has been made that all growth can be regarded as radial. The rationale behind this assumption can be understood by considering the random growth of polymers from an element of the periphery of the domain. Random growth implies that polymers emerge from this element pointed in all directions. Radial growth will arise from the projection of each polymer's growth direction onto a radial direction. If each polymer makes an angle of θ with the radial direction, the growth rate is the product of the maximal growth rate, k_+, times the average over $\cos\theta$ taken for θ between $-\pi/2$ and $\pi/2$. The average growth rate is thus $2k_+/\pi$, and is within a simple factor of order unity of the maximal or bulk rate.

Whereas Eqs. 3, 4, 8, and 9 reduce to the spatially uniform case (Eqs. 1 and 2) if there are no spatial derivatives, integration of these equations over all space need not be equivalent to the uniform case. Because these models are used to determine molecular parameters by fitting to data, a natural question is whether parameters generated by analyzing data with a spatially uniform model (e.g., Eqs. 1) apply to the spatially nonuniform model here (Eqs. 3, 4, 8, and 9). This will be addressed below.

APPROXIMATE SOLUTION

In the absence of an analytic solution to the full system of Eqs. 3, 4, 8, and 9, a perturbation expansion about the initial values (Bishop and Ferrone, 1984) offers considerable insight into the model. As will be shown, the first-order expansion approximates the situation when the concentration of free monomers is taken as fixed at c_0.

To proceed, we observe that of the four variables, the concentration of free monomers, c, is significantly larger than the other concentrations Δ, c_p^+, and c_p^- (at least in the initial stage of polymerization). Thus, we expand c, Δ, c_p^+, and c_p^- in terms of orders of 1, Δ/c, $(\Delta/c)^2$, etc. Of the four variables, c begins as c_0, whereas Δ, c_p^+, and c_p^-

begin as small values. Thus,

$$c = c_0 + c_1 + c_2 + \cdots \tag{11a}$$

$$\Delta = \Delta_1 + \Delta_2 + \cdots \tag{11b}$$

$$c_p^+ = c_{p1}^+ + c_{p2}^+ + \cdots \tag{11c}$$

$$c_p^- = c_{p1}^- + c_{p2}^- + \cdots \tag{11d}$$

Each of the parameters such as J and g must also be expanded about c_0. Substitution and retaining terms of first order gives

$$\frac{\partial c_1}{\partial t} = -\frac{J(c_0)}{2}[c_{p1}^+ + c_{p1}^-] + \frac{D}{r}\frac{\partial}{\partial r}\left(r\frac{\partial c_1}{\partial r}\right) \tag{12a}$$

$$\frac{\partial \Delta_1}{\partial t} = \frac{J(c_0)}{2}[c_{p1}^+ + c_{p1}^-] \tag{12b}$$

$$\frac{\partial c_{p1}^+}{\partial t} = g(c_0)\,\Delta_1 + \frac{\alpha}{r}\frac{\partial}{\partial r}(r\,J(c_0)\,c_{p1}^+) \tag{12c}$$

$$\frac{\partial c_{p1}^-}{\partial t} = g(c_0)\,\Delta_1 - \frac{\alpha}{r}\frac{\partial}{\partial r}(r\,J(c_0)\,c_{p1}^-). \tag{12d}$$

Eqs. 12b–d can be solved separately from Eq. 12a, and are the same as Eqs. 4, 8, and 9 with c replaced by c_0. Physically, this represents the instantaneous replacement of polymerized monomers by monomers which diffuse into the domain. Note that g and J have now become constants, which depend on the initial monomer concentration c_0. The equation for c_1 (Eq. 12a) can be solved once Eqs. 12b–d have been solved. The accuracy of the solutions will be of order c_1/c_0.

To obtain the solutions, it is useful to transform the concentrations $c_p^{\pm}$, c, and Δ, and the coordinates r and t. First, the concentrations are transformed:

$$u = r\,(c_{p1}^+ + c_{p1}^-) \tag{13a}$$

$$v = r\,(c_{p1}^+ - c_{p1}^-) \tag{13b}$$

$$w = r\,\Delta_1 \tag{13c}$$

$$z = r\,c_1. \tag{13d}$$

By substituting u, v, w, and z into Eqs. 12, a new set of equations results. These equations avoid a troublesome singularity at the origin. Moreover, the condition that ingrowing polymers transform to outgrowing polymers at the origin is mathematically established by requiring that $v(0,t) = 0$. At infinite distance, all these variables are assumed to be zero.

The initial conditions are that there are initially two polymer ends, and some small number of polymerized monomers, given by the homogeneous nucleus size i*. Thus, if δ is a delta function in r, the initial condition for u can be written as:

$$u(r, 0) = \frac{1}{\pi N \Delta h}\delta(r), \tag{14a}$$

where N is Avogadro's number, and Δh is the height of the layer in which the domain is viewed. Eq. 14a also specifies $v(r,0)$, because initially $c_p^- = 0$. $w(r,0)$ should be related to the number of nucleated monomers, i*. Thus,

$$w(r, 0) = \frac{\mathrm{i}^*}{2\pi N \Delta h}\delta(r). \tag{14b}$$

However, this initial condition can be replaced by $w(r,0) = 0$ for usual values of the parameters. Inclusion of Eq. 14b adds a term to the solutions of size $(g/J)^{-1/2}$, which is very small. Physically, this says that the effect of having polymer ends which can grow is more significant than having a short initial length of polymer capable of further nucleation on its surface.

Solving the transformed equations is assisted by one further transformation, this time, of the r and t coordinates. Eqs. 12 can be cast into a dimensionless form by using the following change:

$$\tau = \sqrt{gJ}\,t \tag{15a}$$

and

$$\rho = \frac{\sqrt{gJ}}{\alpha J}r. \tag{15b}$$

With this and the transformation of Eqs. 13, the operating Eqs. 12 become:

$$\frac{\partial w}{\partial \tau} = \frac{1}{2}\sqrt{J/g}\,u \tag{16a}$$

$$\frac{\partial u}{\partial \tau} = 2\sqrt{g/J}\,w - \frac{\partial v}{\partial \rho} \tag{16b}$$

$$\frac{\partial v}{\partial \tau} = -\frac{\partial u}{\partial \rho} \tag{16c}$$

$$\frac{\partial z}{\partial \tau} = -\frac{\partial w}{\partial \tau} + \frac{D\sqrt{g/J}}{\alpha^2 J}\frac{\partial}{\partial \rho}\left(\rho\frac{\partial}{\partial \rho}\frac{z}{\rho}\right). \tag{16d}$$

In Eqs. 16a–c only one composite parameter appears, viz., $(g/J)^{1/2}$, which sets the size of w relative to u or v. The solutions to the first three equations (16a–c) are:

$$u(\rho, \tau) = \frac{\sqrt{g/J}}{\pi N \Delta h\,\alpha}\frac{\tau}{\sqrt{\tau^2 - \rho^2}}I_1\left(\sqrt{\tau^2 - \rho^2}\right) \tag{17a}$$

$$v(\rho, \tau) = \frac{\sqrt{g/J}}{\pi N \Delta h \alpha} \frac{\rho}{\sqrt{\tau^2 - \rho^2}} I_1\left(\sqrt{\tau^2 - \rho^2}\right) \quad (17b)$$

$$w(\rho, \tau) = \frac{1}{2\pi N \Delta h \alpha} I_0\left(\sqrt{\tau^2 - \rho^2}\right) \quad (17c)$$

for $\tau > \rho$ and are zero otherwise. I_0 and I_1 are modified Bessel functions (Dwight, 1961). These solutions are shown in Fig. 3.

The accuracy of these solutions depends on the size of c_1/c_0. The smaller c_1/c_0 is, the more accurate are the solutions given by Eq. 17a–c. In the early part of the polymerization process, c_1/c_0 is small. Later on, if diffusion is rapid enough to replenish the monomers which are used in forming polymers, c_1/c_0 can continue to be small. Clearly, such effects of diffusion are greatest near the boundary, where there is a constant supply of free monomers, than near the center.

In Fig. 4 numerical integration of the full equations (Eqs. 3, 4, 8, and 9) and the approximate solution are compared. Two things should be noted. First, the approximate solution provides an excellent description for over two decades. Secondly, the error, as described above, is greater near the center than near the edges.

COMPARISON WITH DATA

There are two main points of comparison between the theoretical predictions of this radial model and experimental data. The most extensive investigations have involved observation of light scattered from a small area, usually in the center of the domain (Ferrone et al., 1985*a*; Hofrichter, 1986), in which it was found that the scattered intensity grew exponentially for times >1 s. In terms of the model presented here, such a measurement represents integrating $\Delta(r, t)$ over a small region about zero. The second measurement involves the study of the spatial dependence of domain growth (Basak et al., 1988), in which domains were parameterized by a gaussian with increasing width. Thus, a comparison of the model with the latter results involves comparing the shape of the domain. These will be examined in turn.

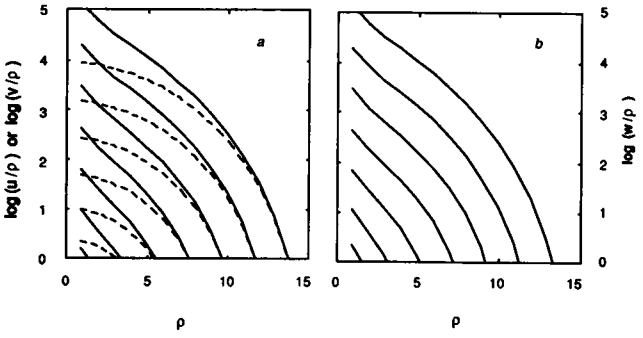

FIGURE 3 Solutions of Eqs. 16a–c, as given by Eqs. 17a–c, which approximate constant concentration of monomers in the domain. Panel *a* shows log (u/ρ) (*solid curve*) and log (v/ρ) (*dashed curve*) as a function of ρ, the dimensionless distance, for different dimensionless times τ, which go from 2 to 15 in increments of two. Dimensionless variables are related to distance and time by Eqs. 15a and b. Panel *b* shows log (w/ρ) as a function of ρ, for different times, as in *a*. The scales in *a* and *b* differ by the factor $(g/J)^{1/2}$, which would make the polymer concentration much smaller; neither scale shows the common prefactor $(\pi N \Delta h \alpha)^{-1/2}$.

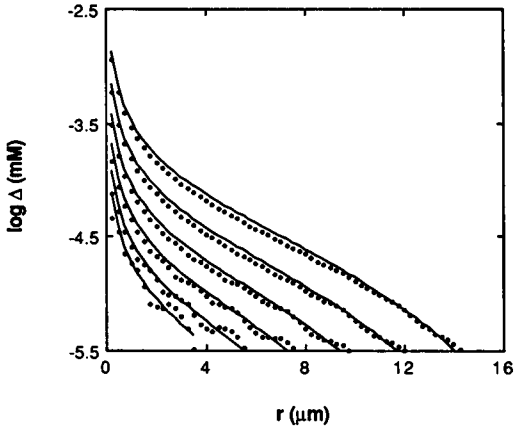

FIGURE 4 Comparison of approximate analytic (*solid curve*) and exact, numerical (*dotted curve*) solutions. Eqs. 3, 4, 8, and 9 were solved numerically using an algorithm based on the Crank-Nicholson scheme (Press et al., 1986) after transforming the variables using Eq. 13. Integrations used a 100-element grid, with each element 0.25 μm in size. Data is shown for 0.02-s time steps. At the boundary (25 μm), the concentration of free monomers, $c(r, t)$, was set equal to the initial concentration and c_p^-, c_p^+, and Δ were set to 0. Because c_p^- must transform to c_p^+ at the origin, c_p^- was transformed into an additional term in c_p^+ at $r = 0$. The integrations began with the first homogeneous nucleus. Initially $c(r, t = 0)$ is set equal to the free monomer concentration at the boundary. The initial value of Δ was taken as zero. Likewise, initially the values of c_p^- was set equal to zero. The concentration of out-growing polymer ends, c_p^+ was set equal to two polymer ends within the first cell. The polymerization parameter values are taken from the 25°C set of Ferrone et al. (1985*a*). D was taken as a constant, equal to 1.13×10^{-7} cm^{2}s^{-1} (Minton and Ross, 1978). The numerical equations were not integrated further to avoid an artifact at the 25-μm boundary, due to the assumption of a large reservoir of monomers just beyond the end of the integration limit. This has no effect on the solution until the domain reaches the integration boundary.

For sample thickness $\Delta h = 6$ μm (Basak et al., 1988), at a radial distance r of 1 μm, the product of the coefficients in

$$\Delta(r, t) = \frac{1}{2\pi N \Delta h \alpha r} I_0\left\{\sqrt{gJ\,[t^2 - (r/\alpha J)^2]}\right\}. \quad (18)$$

Eq. 18 gives a prefactor of ~0.1 μM. Thus, I_0 must be considerable (>100) before polymerization is detected in typical experiments. This in turn requires that the argument for the Bessel function I_0 be >6.5, in which case the asymptotic expression for the modified Bessel function can be employed (Dwight, 1961), viz.,

$$I_0(x) \simeq \frac{e^x}{\sqrt{2\pi x}}. \tag{19}$$

For $x = 6.5$, this is accurate to better than 2% (Abramowitz and Stegun, 1965).

For integration near the origin where r is small, for finite times, $t^2 \gg (r/\alpha J)^2$. In that case, a small parameter expansion gives the further approximation that

$$\Delta(r, t) \simeq \frac{1}{(2\pi)^{3/2} N \Delta h \alpha r (gJ)^{1/4}} \frac{e^{\sqrt{gJ}t}}{\sqrt{t}}. \tag{20}$$

In the integrated experiments, light scattering from a gaussian profile laser beam was employed, thus weighting the different parts of the domain unequally. The observed scattered intensity Φ_{obs} is thus the spatial integral of the product of the polymerized monomer concentration $\Delta(r,t)$ times the intensity at that point, with the integration taken over the region actually viewed. If the laser intensity has gaussian $1/e$ width given by σ, the integral is

$$\Phi_{obs}(t) = 2\pi \Phi_0 \int_0^R \Delta(r,t)\, e^{-(r/\sigma)^2} r\, dr, \tag{21}$$

where R is the aperture size in which the domain is viewed and Φ_0 is the initial intensity times appropriate scattering efficiencies (treated as constant). Using Eq. 20, this becomes

$$\Phi_{obs} = \frac{\Phi_0}{2\sqrt{2} N \Delta h \alpha (gJ)^{1/4}} \frac{e^{\sqrt{gJ}t}}{\sqrt{t}} \sigma\, erf(R/\sigma). \tag{22}$$

This expression is approximately of the form $A\exp(Bt)$, because the $\sqrt{t}$ dependence in the denominator of Eq. 22 is a much weaker time dependence than exponential growth. Thus, we conclude that the model agrees with the observed exponential growth of the integrated data.

In spatially resolved studies of gelation, domains were found to possess approximately gaussian radial profiles (Basak et al., 1988). Subsequent work (Cho and Ferrone, 1990) has shown that the light scattering signal used to characterize those experiments has significant nonlinearities, which cause a substantial decrease in the observed signals before the polymerized hemoglobin has reached its maximum. This being the case, we have allowed for the possibility that the higher concentrations may be in significant error in comparing the predictions of this radial model with the data.

Four parameters have been varied to match the theory to the data: the initiation time, the net growth rate (B), the elongation rate (αJ), and the scattering efficiency. While the latter three are apparent, the need for an initiation time warrants explanation. In a single domain experiment, there is a delay before the observed signal for two reasons. A stochastic delay exists before the homogeneous nucleus is formed, and as the name implies, it is highly variable. This has been extensively studied by Hofrichter (1986). Once the nucleus forms a nonstochastic delay exists before the existence of sufficient polymer mass for observation. This delay is due primarily to the exponential character of the growth process. Experiments on multidomain samples observe the nonstochastic delay. *A priori,* one has no way of distinguishing between the two components of the delay for a single domain experiment. The equations developed here describe domain formation after initiation, and thus do not include the stochastic time. Consequently, to fit the observed data, a variable stochastic delay must be introduced to adjust the time observed to time after initiation. This stochastic delay thus becomes an additional parameter. When this is obtained, the time between the stochastic delay and the first triggered data file will be approximately the delay time or 10th time seen in multidomain experiments.

Fig. 5 compares a typical data set (shown in Fig. 4 of Basak et al., 1988) with Eq. 18. In the fit shown, the stochastic delay is 257.8 s, giving a delay time of 47 s. For the outer four annuli ($r \geq 5$ μm) which generally correspond to lower intensities, the agreement is quite good. Near the origin, the theory predicts a more strongly peaked function where the light scattering signal's linearity is most suspect. We thus conclude that the model displays the correct shape for the domain.

DISCUSSION

The process of sickle hemoglobin gelation has been subject to intense study, first to establish a consistent mechanism for the polymerization, and to determine molecular parameters for use with a successful model. The double nucleation model has provided the most comprehensive explanation for the observed experiments. However, gelation of sickle hemoglobin has a spatial dependence, and the continued description of mechanisms without reference to this dimension is risky (for the description may lead to incorrect results) and restrictive, because the spatial dependence may provide new ways of determining information previously inaccessible. Perhaps most unsettling is the question of whether the unaccounted spatial dependence might invalidate or under-

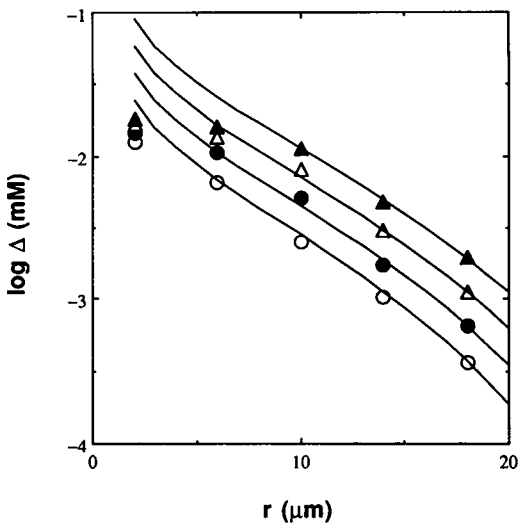

FIGURE 5 Comparison of the approximate solution, given by Eq. 18 (*solid curve*) and data taken from Figs. 4 and 8 of Basak et al. (1988). The sample concentration was 4.86 mM, and the temperature was 11°C. The data points were taken for 310.8 s (*open circles*), 313.8 s (*solid circles*), 316 s (*open triangles*), and 319.8 s (*solid triangles*) after the laser was turned on to initiate the experiment. Four parameters were varied in the fit: the initiation time, the net growth rate (B), the elongation rate (αJ), and the scattering efficiency. The stochastic delay or initiation time was determined to be 257.8 s so that the time when data collection was triggered corresponds to a delay time of 47 s. The first data set shown was collected 53 s after initiation of the domain. The growth rates were: $B = \sqrt{gJ} = 0.154\ s^{-1}$ and $\alpha J = 0.5\ \mu m/s$. Δh was fixed as 6 μm. The scale factor which converts scattered intensity into polymer concentration was also a fit parameter, and allows the ordinate to be labeled in concentration units. The fits were accomplished by attempting to fit only the lower values of log Δ, assuming that the deviations at the higher values (near the domain center) arise from the nonlinearity of response of the light scattering signal.

mine the successes of the model. The description developed here is a first step toward rectifying these deficiencies. First of all, it is clear that the double nucleation mechanism, with suitable spatial generalization, cannot only continue to describe the exponential growth seen in bulk experiments, but also the profiles seen in spatially resolved data. Moreover, this treatment also rationalizes the monomer diffusion we have recently observed (Cho and Ferrone, 1990; Ferrone, 1989).

It is interesting to compare the prediction of a spatially uniform description with the radial model described in this paper. This involves a comparison of the integrated scattering intensity Φ_{obs}. Eq. 22 is thus to be compared with the result obtained from Eqs. 1 and 2, in which nucleation is not spatially dependent but uniform throughout the volume given by $\pi R_0^2 \Delta h$, in which a single nucleus (i.e., two polymer ends) is assumed to have formed. In parallel with Eqs. 21 and 22 above (cf., Hofrichter, 1986), the observed scattering intensity will be given by

$$\Phi_{obs} = \frac{\Phi_0}{NR_0^2 \Delta h} \sqrt{\frac{J}{g}}\, e^{\sqrt{gJ}t}\, \sigma^2 (1 - e^{-(R/\sigma)^2}). \quad (23)$$

Both Eqs. 22 and 23 are approximately exponential and have the same rate constant, hence the assumption of spatial uniformity in Eq. 23 is a good approximation to the correct expression of Eq. 22. Therefore, the rate constant will yield correct molecular parameters $\sqrt{gJ}$. However, the dependence of the prefactor (A) on the molecular parameters is quite different for Eq. 22 and 23. Most notably, in the spatially nonuniform results, the g and J never appear separately, but always as the product gJ indicating that measurements of the integrated intensity alone will not suffice to resolve the g and J as Eq. 23 would have suggested is possible. (J and g can be resolved by stochastic experiments, however [Hofrichter, 1986; Szabo, 1988]). From Eq. 22, if the reaction is parametrized as $A\exp(Bt)$, it is clear that A^2B should be constant for single domains.

The model presented here shows how molecular parameters such as growth rates and nucleation rates can be deduced by analysis of spatially resolved data by explicitly accounting for spatial effects. While a full investigation is still required, the preliminary findings from the fit to the data in Fig. 5 are quite intriguing. The parameter B ($= [gJ]^{1/2}$) is comparable to that found by Ferrone et al. (1985*a*), as is the nonstochastic delay time of 47 s. The smallness of the polymer growth rate J implies a small value for k_+, viz., 9 $mM^{-1}\ s^{-1}$. In data obtained by direct imaging of growing fibers, Samuel et al. (1990) measured a growth rate of 0.3 μm/s, at 28°C for 3.25 mM (tetramer) solutions. This translates into a rate constant of 62 $mM^{-1}\ s^{-1}$, which would be consistent with the slow value deduced here for spatially resolved 11°C data and a 6 kcal/mol apparent activation energy. An apparent weakness of this treatment is that the nonlinearity in the light scattering signal has been assumed to appear abruptly, i.e., the lower points are fit assuming complete linearity. However, the use of the spatial data should be able to overcome the problem of light scattering nonlinearity by examining domains at constant intensity contours. In that case the conversion of $\Delta(r,t)$ to scattering intensity is constant, even if nonlinear in $\Delta(r,t)$. To the degree that the spacing of the intensity contours dominate the fit shown here, to that extent will the results of the fit be insensitive to the nonlinear response of the light scattering. Further work is underway to employ this strategy to determine the various rates for the full data set of Basak et al. (1988).

The incorporation of monomers into polymers must ultimately saturate, and at least two mechanisms can be envisaged which account for this. On the one hand,

polymer–polymer exclusion may simply cap the concentration of monomers that can become polymers. On the other hand, the density of polymers may affect the diffusion constant, assumed constant here. Neither mechanism is successfully incorporated into this model yet, and until that is done, the accurate representation of the saturation of domain growth will be beyond the scope of this treatment.

Finally, the approach taken here could also be used for other polymer forming molecules, such as actin or tubulin, even though the details of the polymerization process (g and J functions) would differ. Although those systems do not form polymer domains per se, they do typically polymerize from intracellular nucleating centers, which formally would be equivalent to the center of the domain as used here. Perhaps most usefully, this model provides a framework for describing concentration gradients due to sinks in such polymer formation processes.

This work was supported by the National Institutes of Health, through grant HL28102.

Received for publication 15 September 1989 and in final form 19 March 1990.

REFERENCES

Abramowitz, M., and I. A. Stegun. 1965. Handbook of Mathematical Functions. Dover Press, New York.

Basak, S., F. A. Ferrone, and J. T. Wang. 1988. Kinetics of domain formation by sickle hemoglobin polymers. *Biophys. J.* 54:829–843.

Beach, D. A., C. Bustamante, K. S. Wells, and K. M. Foucar. 1988. Differential polarization imaging. III. Theory confirmation. Patterns of polymerization of hemoglobin S in red blood cells. *Biophys. J.* 53:449–456.

Bishop, M. F., and F. A. Ferrone. 1984. Kinetics of nucleation controlled polymerization: a perturbation treatment for use with a secondary pathway. *Biophys. J.* 46:631–644.

Cho, M. R., and F. A. Ferrone. 1990. Monomer diffusion into polymer domains in sickle hemoglobin. *Biophysical. J.* In press.

Dwight, H. B. 1961. Tables of Integrals and Other Mathematical Data. 4th ed. Macmillan Publishing Co., New York.

Dykes, G., R. H. Crepeu, and S. J. Edelstein. 1978. Three dimensional reconstruction of the fibres of sickle cell haemoglobin. *Nature (Lond.).* 272:506–510.

Eaton, W. A., and J. Hofrichter. 1978. Successes and failures of a simple nucleation theory for sickle cell hemoglobin gelation. *In* Biochemical and Clinical Aspects of Hemoglobin Abnormalities. W. S. Caughey, editor. Academic Press Inc., New York. 443–457.

Ferrone, F. A. 1989. Kinetic models and the pathophysiology of sickle cell disease. *Ann. NY Acad. Sci.* 565:63–74.

Ferrone, F. A., J. Hofrichter, H. Sunshine, and W. A. Eaton. 1980. Kinetic studies on photolysis-induced gelation of sickle cell hemoglobin suggest a new mechanism. *Biophys. J.* 32:361–377.

Ferrone, F. A., J. Hofrichter, and W. A. Eaton. 1985*a*. Kinetics of sickle hemoglobin polymerization. I. Studies using temperature-jump and laser photolysis techniques. *J. Mol. Biol.* 183:591–610.

Ferrone, F. A., J. Hofrichter, and W. A. Eaton. 1985*b*. Kinetics of sickle hemoglobin polymerization. II. A double nucleation mechanism. *J. Mol. Biol.* 183:611–631.

Ferrone, F. A., S. Basak, A. J. Martino, and H. X. Zhou. 1987. Polymer domains, gelation models and sickle cell crises. *In* Pathophysiological Aspects of Sickle-Cell Vaso-Occlusion. R. Nagel, editor. Alan R. Liss, Inc., New York. 47–58.

Firestone, M. P., S. K. Rangarajan, and R. deLevie. 1983. On one-dimensional nucleation and growth of "living" polymers. I. Homogeneous nucleation. *J. Theor. Biol.* 104:535–552.

Goldstein, R. F., and L. Stryer. 1986. Cooperative polymerization reactions. Analytical approximations, numerical examples and experimental strategy. *Biophys. J.* 50:583–600.

Hofrichter, J. 1979. Ligand binding and the gelation of sickle cell hemoglobin. *J. Mol. Biol.* 128:335–369.

Hofrichter, J. 1986. Kinetics of sickle hemoglobin polymerization. III. Nucleation rates determined from stochastic fluctuations in polymerization progress curves. *J. Mol. Biol.* 189:553–571.

Hofrichter, J., P. D. Ross, and W. A. Eaton. 1974. Kinetics and mechanism of deoxyhemoglobin S gelation: a new approach to understanding sickle cell disease. *Proc. Natl. Acad. Sci. USA.* 71:4864–4868.

Hofrichter, J., P. D. Ross, and W. A. Eaton. 1976. A physical description of hemoglobin S gelation. *In* Proceedings of the Symposium on Molecular and Cellular Aspects of Sickle Cell Disease. J. I Hercules, G. L. Cottam, M. R. Waterman, and A. N. Schechter, editors. Department of Health, Education and Welfare publication NIH 76-1007. 185–224.

Kam, Z., and J. Hofrichter. 1986. Quasi-elastic laser light scattering from solutions and gels of hemoglobin S. *Biophys. J.* 50:1015–1020.

Malfa, K., and J. Steinhardt. 1974. A temperature dependent latent period in the aggregation of sickle hemoglobin *Biochem. Biophys. Res. Commun.* 59:887–893.

Mickols, W., M. F. Maestre, I. Tinoco, and S. H. Embury. 1985. Visualization of oriented hemoglobin S in individual erythrocyte by differential extinction of polarized light. *Proc. Natl. Acad. Sci. USA.* 82:6527–6531.

Mickols, W., J. D. Corbett, M. F. Maestre, I. Tinoco, J. Kropp, and S. H. Embury. 1988. The effect of speed of deoxygenation of the percentage of aligned hemoglobin in sickle cells. Application of differential polarization microscopy. *J. Biol. Chem.* 263:4338–4346.

Minton, A. P., and P. D. Ross. 1978. Concentration dependence of the diffusion coefficient of hemoglobin. *J. Phys. Chem.* 82:1934–1938.

Oosawa, F., and S. Asakura. 1975. Thermodynamics of the Polymerization of Protein. Academic Press, Inc., New York.

Press, W. H., B. P. Flannery, S. A. Teukolsky, and W. T. Vetterling. 1986. Numerical Recipes. Cambridge University Press, Cambridge.

Rangarajan, S. K., and R. de Levie. 1983. On one-dimensional nucleation and growth of "living" polymers. II. Growth constant monomer concentration. *J. Theor. Biol.* 104:553–570.

Samuel, R. E., E. D. Salmon, and R. W. Briehl. 1990. Direct observation of nucleation, growth and gelation of sickle cell hemoglobin (HbS) by video enhanced differential interference contrast (DIC) microscopy. *Biophys. J.* 57:229a. (Abstr.)

Sunshine, H. R., J. Hofrichter, F. A. Ferrone, and W. A. Eaton. 1982. Oxygen binding by sickle cell hemoglobin polymers. *J. Mol. Biol.* 158:251–273.

Szabo, A. 1988. Fluctuations in the polymerization of sickle hemoglobin: a simple analytical model. *J. Mol. Biol.* 199:539–542.

White, J. G., and B. Heagan. 1970. The fine structure of cell free sickled hemoglobin. *Am. J. Pathol.* 58:1–17.